



저작자표시-비영리-변경금지 2.0 대한민국

이용자는 아래의 조건을 따르는 경우에 한하여 자유롭게

- 이 저작물을 복제, 배포, 전송, 전시, 공연 및 방송할 수 있습니다.

다음과 같은 조건을 따라야 합니다:



저작자표시. 귀하는 원저작자를 표시하여야 합니다.



비영리. 귀하는 이 저작물을 영리 목적으로 이용할 수 없습니다.



변경금지. 귀하는 이 저작물을 개작, 변형 또는 가공할 수 없습니다.

- 귀하는, 이 저작물의 재이용이나 배포의 경우, 이 저작물에 적용된 이용허락조건을 명확하게 나타내어야 합니다.
- 저작권자로부터 별도의 허가를 받으면 이러한 조건들은 적용되지 않습니다.

저작권법에 따른 이용자의 권리는 위의 내용에 의하여 영향을 받지 않습니다.

이것은 [이용허락규약\(Legal Code\)](#)을 이해하기 쉽게 요약한 것입니다.

[Disclaimer](#)

工學碩士 學位論文

군함에서의 추적모듈용 $\alpha-\beta-\gamma$ 필터와
칼만 필터의 성능비교에 관한 연구

A Study on the Performance Comparison of $\alpha-\beta-\gamma$
Filter and Kalman Filter for a Tracking Module on
board High Dynamic Warships



指導教授 鄭 泰 權

2016年 12月

韓國海洋大學校 大學院

航海學科

NJONJO ANNE WANJIRU

本 論文을 NJONJO ANNE WANJIRU의 工學碩士
學位論文으로 認准함.

委員長 工學博士 芮 秉 德 (印)

委 員 工學博士 文 星 培 (印)

委 員 工學博士 鄭 泰 權 (印)



2016年 12月 22日

韓國海洋大學校 大學院

We approved this dissertation submitted by NJONJO ANNE WANJIRU for the requirement of Master's Degree of Engineering

Chairman of Supervisory Committee Byeong-Deok, Yea (Seal)

Member of Committee Serng-Bae, Moon (Seal)

Member of Committee Tae-Gweon, JEONG (Seal)



22nd December, 2016

Graduate School of Korea Maritime And Ocean University

本 論文을 NJONJO ANNE WANJIRU의 工學碩士
學位論文으로 認准함.

委員長 工學博士 芮 秉 德



委 員 工學博士 文 星 培



委 員 工學博士 鄭 泰 權



2016年 12月 22日

韓國海洋大學校 大學院

We approved this dissertation submitted by NJONJO ANNE WANJIRU for the requirement of Master's Degree of Engineering

Chairman of Supervisory Committee Byeong-Deok, Yea



Member of Committee Serng-Bae, Moon



Member of Committee Tae-Gweon, JEONG



22nd December, 2016

Graduate School of Korea Maritime And Ocean University

Contents

| | |
|---|-----|
| List of Tables | iii |
| List of Figures | iv |
| Abstract | vii |
| | |
| Chapter 1. Introduction | 1 |
| 1.1 Scope | 1 |
| 1.2 Literature | 2 |
| 1.2.1 Role of a Filter in a Physical System | 2 |
| 1.2.2 Literature Review | 3 |
| 1.3 Methodology and Contents | 6 |
| | |
| Chapter 2. Theory of Tracking Filters | 8 |
| 2.1 Theory of α-β-γ Tracking Filter | 8 |
| 2.1.1 Benedict-Bordner model | 10 |
| 2.1.2 Gray-Murray model | 10 |
| 2.1.3 The Fading memory model | 11 |
| 2.2 Theory of the Kalman Filter | 12 |
| | |
| Chapter 3. Simulation | 15 |
| 3.1 Initial Input of Target Dynamics | 15 |

| | | |
|---|---|-----------|
| 3.2 | Input Motion Model of the Target Dynamics | 15 |
| 3.3 | Noise Modelling..... | 16 |
| 3.4 | α - β - γ Filter Weights Selection and Computation..... | 17 |
| 3.4.1 | Filter Gain Coefficient Selection Using Benedict-Bordner Model..... | 17 |
| 3.4.2 | Filter Gain Coefficient Selection Using Gray-Murray Model..... | 18 |
| 3.4.3 | Filter Gain Coefficient Selection Using Fading Memory Model | 20 |
| 3.4.3.1 | Fading memory model Optimization..... | 22 |
| 3.4.3.1.1 | Optimization by Position..... | 23 |
| 3.4.3.1.2 | Optimization by Velocity and Acceleration..... | 28 |
| 3.5 | Kalman Filter Tuning..... | 31 |
| 3.5.1 | Q Covariance Matrix Tuning..... | 31 |
| 3.5.2 | R Covariance Matrix Tuning..... | 33 |
| 3.6 | Result Analysis and Discussion | 34 |
| 3.6.1 | α - β - γ Filter Results and Remarks | 34 |
| 3.6.2 | Kalman Filter Results and Remarks | 40 |
| 3.6.2 | Kalman Filter vs. α - β - γ Filter | 42 |
| Chapter 4. Conclusion and Future Prospects | | 44 |
| Reference..... | | 47 |
| Acknowledgments..... | | 49 |

List of Tables

| | | |
|------------------|--|----|
| Table 3.1 | Summary of Initial Input of Target Dynamics | 15 |
| Table 3.2 | Smoothing Coefficients Obtained from Benedict-Bordner Model .. | 18 |
| Table 3.3 | Smoothing Coefficients Obtained from Gray-Murray Model..... | 20 |
| Table 3.4 | Optimal ξ for Different Initial Velocities | 30 |
| Table 3.5 | Smoothing Coefficients Obtained from Fading Memory Model | 31 |
| Table 3.6 | Variance Reduction Ratios..... | 40 |
| Table 3.7 | Total Tracking and Estimation Accuracies | 43 |



List of Figures

| | | |
|--------------------|---|----|
| Figure 1.1 | General Filter Application on a Physical System | 3 |
| Figure 3.1 | Target's True Trajectory | 16 |
| Figure 3.2 | East-West Observation Error | 16 |
| Figure 3.3 | North-South Observation Error..... | 17 |
| Figure 3.4 | Residual between observed and predicted positions against corresponding value of α | 18 |
| Figure 3.5 | Cumulative error difference between observed and predicted positions against maneuverability error variance..... | 19 |
| Figure 3.6 | Cumulative error difference between true and smoothed positions against maneuverability error variance | 19 |
| Figure 3.7 | Cumulative error difference between observed and predicted positions against measurement error variance | 20 |
| Figure 3.8 | Cumulative error difference between true and smoothed positions against measurement error variance..... | 20 |
| Figure 3.9 | Target's True, Observed, Predicted and Smoothed Position, ($\xi=0.2$)..... | 21 |
| Figure 3.10 | Target's True, Observed, Predicted and Smoothed Position, ($\xi=0.8$)..... | 22 |
| Figure 3.11 | Target's True, Observed, Predicted and Smoothed Position, ($\xi=0.64$)..... | 22 |
| Figure 3.12 | Target's True, Observed, Predicted and Smoothed Position, ($\xi=0.5$)..... | 23 |

| | | |
|--------------------|--|----|
| Figure 3.13 | Enlarged View of target's True, Observed, Predicted and smoothed Position ($\xi=0.5$) corresponding to Fig. 3.12..... | 24 |
| Figure 3.14 | Difference between the true and predicted positions corresponding to Fig. 3.12 | 24 |
| Figure 3.15 | Difference between the true and smoothed positions corresponding to Fig. 3.12 | 25 |
| Figure 3.16 | Summation of residual error T-P for varying ksi..... | 26 |
| Figure 3.17 | Summation of the error difference between true and predicted positions for varying values of ζ after 30 simulation runs | 27 |
| Figure 3.18 | Summation of the error difference between true and predicted positions for average values of summation for each ksi corresponding to Fig. 3.16 | 27 |
| Figure 3.19 | Summation of the error difference between true and smoothed Positions for average values of ζ after 30 simulation runs | 27 |
| Figure 3.20 | Average cumulative error between true and smoothed velocity for each value of ζ after 30 simulation runs..... | 29 |
| Figure 3.21 | Average cumulative error between true and smoothed acceleration for each value of ζ after 30 simulation runs..... | 29 |
| Figure 3.22 | Cumulative error difference between observed and predicted positions against Q matrix coefficient | 32 |
| Figure 3.23 | Cumulative error difference between true and smoothed positions against Q matrix coefficient..... | 32 |
| Figure 3.24 | Cumulative error difference between observed and predicted positions against R matrix coefficient..... | 33 |

| | | |
|--------------------|--|----|
| Figure 3.25 | cumulative error difference between true and smoothed positions against R matrix coefficient | 33 |
| Figure 3.26 | Target's True, Observed, Predicted and Smoothed Position, Benedict-Bordner model | 35 |
| Figure 3.27 | Target's True, Observed, Predicted and Smoothed Position, Gray-Murray model..... | 36 |
| Figure 3.28 | Target's True, Observed, Predicted and Smoothed Position Fading Memory model, ($\xi=0.64$) | 36 |
| Figure 3.29 | Total prediction error, Benedict-Bordner model..... | 37 |
| Figure 3.30 | Total prediction error, Gray-Murray model..... | 38 |
| Figure 3.31 | Total prediction error, Fading memory model..... | 38 |
| Figure 3.32 | Total estimation error, Benedict-Bordner model | 38 |
| Figure 3.33 | Total estimation error, Gray-Murray model | 39 |
| Figure 3.34 | Total estimation error, Fading memory model | 39 |
| Figure 3.35 | Target's True, Observed, Predicted and Smoothed Position, Kalman Filter | 41 |
| Figure 3.36 | Total prediction error, Kalman filter | 41 |
| Figure 3.37 | Total estimation error, Kalman filter | 42 |

A Study on the Performance Comparison of α - β - γ Filter and Kalman Filter for a Tracking Module on Board High Dynamic Warships

Njonjo, Anne Wanjiru

Department of Navigation Science

Graduate School of Korea Maritime and Ocean University

Busan Korea

Abstract

Tracking refers to the estimation of the state of a target on motion with some degree of accuracy given at least one measurement. The measurement, which is the output obtained from sensors, contains system errors and errors resulting from the surrounding environment. Tracking filters play the key role of target state estimation after which the tracking system is updated. Therefore, the type of filter used in carrying out the estimations is crucial in determining the integrity and reliability of the updated value. This is especially true since different filters vary in their performance when subjected to different environments and initial conditions of motion dynamics. In addition, applications of different filter design methods have previously confirmed that filtering performance is a tradeoff between error reduction and a good transient response. Therefore, the criteria for selecting a particular filter for use in a tracking application depends on the given performance requirement.

This study explores and investigates the operation of the Kalman filter and three α - β - γ tracking filter models that include Benedict-Bordner also known as the Simpson filter, Gray-Murray model and the fading memory α - β - γ filter. These

filters are then compared based on the ability to reduce noise and follow a high dynamic target warship with minimum total lag error. The total lag error is the cumulative residual error computed from the difference between the true and the predicted positions, and the true and estimated positions for the given data samples. The results indicate that, although the Benedict-Bordner model performs poorly compared to the other filters in all aspects of performance comparison, the filter starts off sluggishly at the beginning of the tracking process as indicated by the overshooting on the trajectories, but stabilizes and picks up a good transient response as the tracking duration increases. The Gray-Murray model, on the other hand, demonstrates a better tracking ability as depicted by its higher accuracy and an even better response to a change in the target's maneuver as compared to the Benedict-Bordner model. The Fading memory model out-performs the other two α - β - γ filters in terms of tracking and estimation error reduction, but based on sensitivity to target maneuvers and variance reduction ratio the Gray-Murray model demonstrates a slightly better performance. The Kalman filter, on the other hand, has a higher tracking accuracy compared to the α - β - γ filters which, however, have a higher sensitivity to target maneuvers and data stability as indicated by the steadier trajectories obtained. These results are a further proof that no one particular filter is perfect in all dimensions of selection criteria but it is rather a compromise that has to be made depending on the requirement of the physical system under consideration.

Key words: α - β - γ filters, Kalman filter, performance comparison, tracking accuracy, stable response

Chapter 1. Introduction

1.1 Scope

The tracking radar system has a wide application in both the military and civilian fields. In the military, tracking is essential for air traffic control, fire control and missile guidance and target interception during defensive situations, whereas in commercial application it is useful for not only controlling traffic of manned maneuverable vehicles such as ships, submarines and aircrafts which require accurate tracking, but also for collision avoidance.

A high dynamic warship is defined by high speed and quick maneuvering characteristics. Therefore, prompt and accurate estimations of the dynamic parameters is essential for a high degree of precision in tracking in order to make well calculated decisions especially in defensive situations. A variety of algorithms differing in implementation complexities have been developed over the years in order to realize the tracking process which involves the use of special filters to aid in noise reduction hence achieving accurate predictions. Some of the tracking filters in use today in many tracking applications are the Kalman filter and α - β - γ filter where the latter is an extension of the α - β filter aimed at tracking an accelerating target since the α - β filter is only effective when the target model input is a constant velocity.

This research aims to compare the performance of the filters employed to track a high dynamic warship from a stationary own ship. The comparison criteria involves comparing the filters' capability to reduce noise and steadily follow the highly maneuvering target. The Kalman filter and three α - β - γ filter algorithms have been investigated and discussed. The α - β - γ filters include the Benedict-Bordner model which is also known as the Simpson filter, Gray-Murray model and the fading memory α - β - γ filter (critically damped filter). The four filtering

algorithms are executed under similar initial conditions for a target model moving at a high speed and possessing quick maneuvering characteristics. The simulation results are then obtained and subsequently performance comparison is carried out. The critically damped filter was optimized by adjusting the value of the discounting parameter, ξ , experimentally where it was explicitly noted that the optimum set of the smoothing coefficients depends on the initial speed and average speed of the target under consideration. The details regarding the optimization procedure are further discussed in Chapter 3. The Kalman filter employed in this study uses fixed values of the measurement and maneuverability noise covariance R and Q respectively which were carefully selected and tuned to avoid divergence of the data samples.

The subsequent sections of this chapter include a brief description of the role of a filter in a physical process followed by a study on the literature review based on previous researches regarding tracking filters.

1.2 Literature

1.2.1 The role of a filter in a physical system

External inputs and controls are the driving elements of a given physical system such as radar tracking system, inertial navigation system, GPS, chemical plant etc.

Outputs of such a system are provided by measuring devices or sensors. Therefore, the system's behaviour can be evaluated and understood through the inputs and observed outputs. However, since no known system is error-free, the observation contains errors, leading to uncertainties, obtained from the measuring devices of the system. The observed measurement provides the input, which can be in the form of a position measurement and a measurement noise, to a filter

which then plays the key role of obtaining an estimate of the desired system's state that enhances the system's performance based on a given design requirement.

The flow chart in Fig. 1.1 illustrates the typical filtering problem where the filter in this case can be either α - β - γ or Kalman filter.

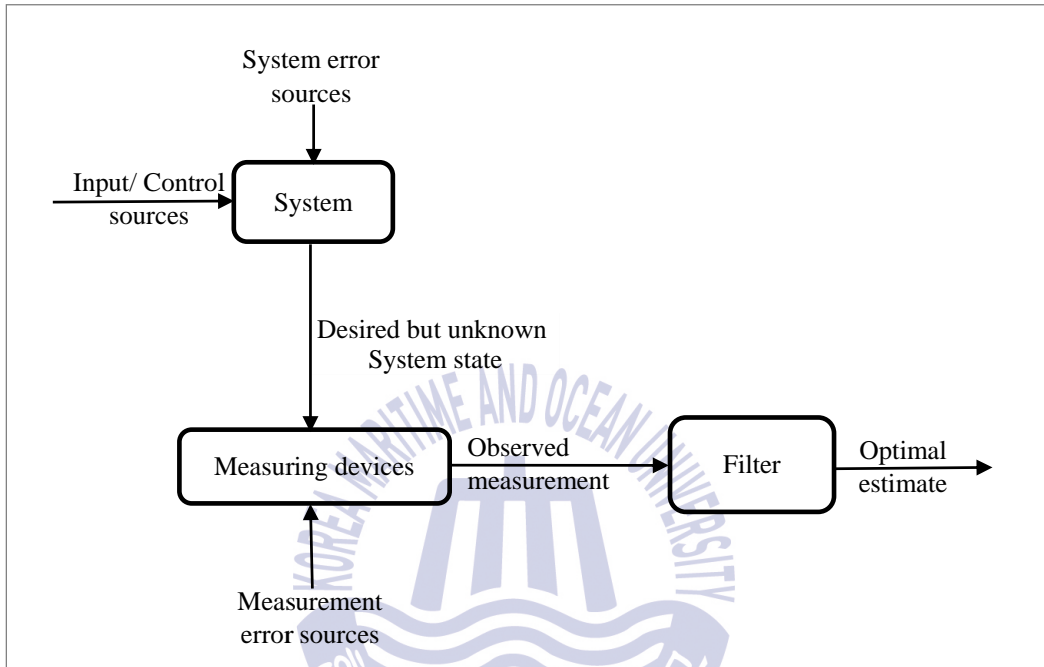


Fig. 1.1 Block diagram of filter application on a physical system
<Adapted from Maybeck, 1990>

In this study, the tracking filter algorithms are incorporated into the control loop of the processor which employs the observed measurements obtained from a track-while-scan (TWS) radar that performs the tracking of targets as the antennae rotates at a constant rate of 20 RPM searching the vicinity for target acquisition.

1.2.2 Literature Review

The role that tracking filters play in an automatic target tracking system cannot be overemphasized. This has led to, in the recent past, a rise in the number of

research work that is heavily invested in their improvement, particularly the performance of the α - β - γ and Kalman filters due to their diverse applications in many fields, which has consequently resulted in the adoption of a wide range of valuable insights for the purpose of their design enhancement.

Benedict et al (1962) carried out an analysis of the α - β filter based on the frequency domain (Z- transform). The study proposed a relationship between the α and β filtering coefficients derived from a pole matching technique in order to optimize the tracker's ability to reduce noise and achieve a good transient performance. This led to what is today known as the Benedict-Bordner model relationship. Simpson (1963) further extended this study to the α - β - γ filter by including the constant acceleration term thus arriving at the optimization condition between the filtering coefficients.

Kalata (1984) proposed the use of a tracking index which relates the filter coefficients and is a function of position uncertainty due to target maneuverability, radar measurement uncertainty and update time interval. He utilized the tracking index parameter to derive implicit closed form equations of the smoothing coefficients which resulted in optimal performance. Later, Gray et al (1993) presented a more convenient way to determine the optimal filtering weights whereby a damping parameter that computes the position smoothing coefficient directly was derived analytically from the Kalata tracking index.

Tenne et al (2002) derived closed form solutions of an optimal α - β - γ filter whose performance was based on noise reduction ratio, steady state maneuver error and transient response for circular and straight line trajectories and subsequently determining a figure of demerit.

Njonjo et al (2016) investigated the performance of the fading memory α - β - γ filter on a high dynamic warship. The research concluded that the filter was capable of tracking the highly maneuvering vessel with an acceptable level of

accuracy in terms of noise reduction. Pan et al (2016) further extended this research where the filter was optimized in order to improve its tracking ability by reducing the noise further and achieving a better precision in prediction. The optimization procedure involved varying the value of the discounting factor, ξ , with the sum of the residual error and determining the ξ that corresponded to the minimum error. The study demonstrated that the optimal filter uniquely varies with the initial speed and average speed of the target under consideration.

Various researchers have dedicated their time in carrying out performance comparison of different filter design methods based on a variety of differing criteria for comparison. Lawton et al (1998) distinguishes among four types of filtering methods including α - β filter, augmented α - β filter, linear Kalman filter and extended Kalman filter for tracking a non-maneuvering target. All the four filters examined are shown to yield the same results when tested under benign condition in which all measurement data is available. Under conditions in which huge portions of the measurements are lost, the extended Kalman filter produces better estimates compared to the other filters.

Blair et al (1991) compares the two-stage α - β - $\bar{\gamma}$ filter estimator with the standard α - β filter and α - β - γ filter in tracking a maneuvering target whereby the results indicate that the two-stage α - β - $\bar{\gamma}$ estimator performs better in the tracking of maneuvering targets hence have increased potential for tracking targets within combat systems that are responsible for tracking and engaging a large number of targets.

The Kalman filter aims to minimize the mean squared error as long as target dynamics are modelled accurately. It makes optimal use of the target measurements by adjusting the filter weights to take into account the accuracy of the n th measurement as described by Brookner (1998). Therefore, the optimal values of the smoothing parameters are dependent on the n th sample.

This study aims to compare the performance of the Benedict-Bordner α - β - γ filter model, the Gray-Murray model, the Fading memory model and Kalman filter for tracking a high dynamic warship from a stationary own ship. The comparison criteria involves comparing the filter's capability to reduce noise and steadily follow a maneuvering target. In this study, the fading memory α - β - γ filter used is an optimal filter whose optimization procedure involved fine-tuning the damping parameter the result of which determines the α , β and γ filtering coefficients as discussed in Chapter 3. The Kalman filter employed in this study uses fixed values of the measurement and dynamic noise covariance R and Q respectively which were determined and selected through an iterative trial and error method in order to arrive at the best values that meet the requirements of sensitivity to target maneuvers and noise reduction.

1.3 Methodology and Contents

This thesis carries out the analysis of three α - β - γ tracking filters and the Kalman filter by comparing their tracking performance. The performance is based on three design requirements as follows;

- i. Tracking and estimation error reduction,
- ii. Sensitivity to target maneuvers and output data stability and,
- iii. Variance reduction ratio (VRR).

Tracking and estimation error reduction capability is determined by computing the total residual obtained from the deviation from the true positions to the prediction and estimation positions respectively for the given sample for each filter design method. The filter design method that results in the smallest residual is considered to out-perform the others in this respect.

With regard to ability to follow target maneuvers with sensitivity and possess output data stability in this study, trajectories are observed for fluctuations and

overshooting at various points thus depicting the filter's stability and ability to steadily track the desired signal as close as possible.

In addition, the variance reduction ratio (VRR), a measure of the measurement error reduction is computed from the ratio of the root mean square noise output to the root mean square noise input which are functions of the filtering weights (Mahafza et al, 2004). Eq. (1.1) represent the variance reduction in the position, Eq. (1.2) is the variance reduction ratio in the velocity, and Eq. (1.3) shows the variance reduction ratio in the acceleration. The filter design method resulting in the smallest values is said to perform better in terms of measurement noise reduction.

$$(VRR)_x = \frac{2\beta(2\alpha^2+2\beta-3\alpha\beta)-\alpha\gamma(4-2\alpha-\beta)}{(4-2\alpha-\beta)(2\alpha\beta+\alpha\gamma-2\gamma)} \quad (1.1)$$

$$(VRR)_{\dot{x}} = \frac{4\beta^3-4\beta^2\gamma+2\gamma^2(2-\alpha)}{t^2(4-2\alpha-\beta)(2\alpha\beta+\alpha\gamma-2\gamma)} \quad (1.2)$$

$$(VRR)_{\ddot{x}} = \frac{4\beta\gamma^2}{t^4(4-2\alpha-\beta)(2\alpha\beta+\alpha\gamma-2\gamma)} \quad (1.3)$$

The rest of this research is organized as follows; chapter two contains the theory of tracking filters that have been considered for this study; Chapter three includes the simulation of the desired motion signal and the results and discussion and; finally chapter four contains the concluding remarks and further research on this topic.

Chapter 2. Theory of Tracking Filters

2.1 Theory of α - β - γ Tracking Filter

α - β - γ filter is a constant gain, three- state tracking filter where the three state vector includes position, velocity and acceleration. The acceleration is assumed to be constant and includes zero mean white Gaussian noise. The filter is easy to design and implement due to its low computational load as it has only three design parameters, that is α , β and γ , from which the performance indices, such as filter stability and tracking ability, can be evaluated. In addition, the smoothing coefficients of the filter are constant for a given sensor which further contributes to its design simplicity. As a result, it has been applied to many tracking systems.

The algorithm involves two major stages of computations, that is, prediction and smoothing (Mahafza et al, 2004). Prediction is performed through execution of Eq. (2.1) for position, Eq. (2.2) for velocity and Eq. (2.3) for acceleration where the respective states are updated from the estimated (smoothed) state thereby attenuating the tracking error.

Prediction equations;

$$P_P(n) = P_S(n - 1) + tV_S(n - 1) + \frac{t^2}{2}A_S(n - 1) \quad (2.1)$$

$$V_P(n) = V_S(n - 1) + tA_S(n - 1) \quad (2.2)$$

$$A_P(n) = A_S(n - 1) \quad (2.3)$$

Eq. (2.4) is the smoothing equation for position, Eq. (2.5) for velocity and Eq. (2.6) represents the smoothing equation for acceleration. These equations are used

to obtain the updated target's states and are computed by adding a weighted difference between the observed position and the predicted position to the forecast state.

Smoothing equations;

$$P_s(n) = P_p(n) + \alpha(P_o(n) - P_p(n)) \quad (2.4)$$

$$V_s(n) = V_p(n) + \frac{\beta}{t}(P_o(n) - P_p(n)) \quad (2.5)$$

$$A_s(n) = A_p(n) + \frac{2\gamma}{t^2}(P_o(n) - P_p(n)) \quad (2.6)$$

Definition of terms

- (1) the predicted target position is denoted by P_p ,
- (2) the predicted target velocity is denoted by V_p ,
- (3) the predicted target acceleration is denoted by A_p ,
- (4) the smoothed target position is denoted by P_s ,
- (5) the smoothed target velocity is denoted by V_s ,
- (6) the smoothed target acceleration is denoted by A_s ,
- (7) the target observed position is denoted by P_o ,
- (8) t is the simulation time interval and
- (9) n is the sample number.

The selection of the weighting coefficient is an important design consideration as it directly affects the stability of the output data, error reduction capability and other key design parameters. The theory and operation of the three optimal α - β - γ filter designs and Kalman filter are explained in the next sub-section. The three designs of the α - β - γ filter differ in their selection and subsequent computation process of the smoothing coefficients α , β and γ .

2.1.1 Benedict-Bordner Model

This was the first optimal tracking filter to be derived. The relationship fixed beta in terms of alpha as shown in Eq. (2.7) (Benedict et al, 1962);

$$\beta = \frac{\alpha^2}{2-\alpha} \quad (2.7)$$

The design of this filter does not specify the optimal position smoothing coefficient, α , hence it is chosen based on the system application. It is, however, proposed to vary α with observed high frequency power fluctuations of the tracking error residual or the innovation, $(P_o(n) - P_p(n))$.

The Benedict-Bordner model coefficient relationship becomes an optimal third order tracking filter when the condition shown in Eq. (2.8) is satisfied according to Simpson (1963).

$$2\beta - \alpha \left(\alpha + \beta + \frac{\gamma}{2} \right) = 0 \quad (2.8)$$

2.1.2 Gray-Murray Model

This filter is an extension of the Kalata filter coefficients relationship which employs the tracking index to compute a damping parameter which is consequently used to calculate the position smoothing coefficient, α . The tracking index is given by the relationship shown in Eq. (2.9) as derived by Kalata (1983).

$$\Lambda = \frac{t^2 \sigma_w}{\sigma_v} \quad (2.9)$$

where t , σ_w and σ_v are the target tracking period, maneuverability and measurement noise respectively.

The damping parameter, r , is computed as shown in Eq. (2.10) and the gain parameters α , β , and γ , are obtained explicitly as shown in Eq. (2.11) for position smoothing coefficient, Eq. (2.12) for velocity smoothing coefficient and (2.13) for the acceleration smoothing coefficient (Gray et al, 1993).

$$r = \frac{(4+\Delta) - \sqrt{8\Delta + \Delta^2}}{4} \quad (2.10)$$

$$\alpha = 1 - r^2 \quad (2.11)$$

$$\beta = 2(2 - \alpha) - 4\sqrt{1 - \alpha} \quad (2.12)$$

$$\gamma = \frac{\beta^2}{2\alpha} \quad (2.13)$$

2.1.3 The Fading Memory Model

The fading memory model has three real roots and represents the filter minimizing the discounted old data least squares error for a constantly accelerating target as discussed by Brookner (1998). The position, velocity and acceleration gain coefficients are determined by the damping parameter, ξ , which is the discounting factor and whose value was selected through an optimization process and found to depend on the initial and average speed of the target under consideration as discussed further in Chapter 3. The smoothing coefficients are computed as shown in Eq. (2.14) for position smoothing coefficient, Eq. (2.15) for velocity smoothing coefficient and (2.16) for the acceleration smoothing coefficient.

$$\alpha = 1 - \xi^3 \quad (2.14)$$

$$\beta = 1.5(1 - \xi)^2(1 + \xi) \quad (2.15)$$

$$\gamma = (1 - \xi)^3 \quad (2.16)$$

2.2 Theory of the Kalman Filter

In the introduction of the Kalman filter, Kalman (1960) described it as a recursive solution to the discrete-data linear filtering problem. A recursive filter is one that requires very little data storage as only the incoming data information is used and therefore does not store up previous information. In addition, the recursive attribute of the Kalman filter ensures that new measurements can be processed as they arrive. It is known to be a good optimal linear estimator in the sense that if the noise is White Gaussian noise, it minimizes the mean square error estimate of the random vector that is the system's state. However, the filter is fundamentally not designed to handle maneuvering targets.

The basic concept of the Kalman filter comprises the following steps;

Prediction step;

Eq. (2.17) is the state prediction equation as it predicts the state of the target at time $t+1$ based on the state at time t . Eq. (2.18) is the predicted state covariance matrix of the process noise w_t and it depicts the accuracy of predicting the target's state at time $t+1$ based on the state values obtained at time t .

$$X_{t+1} = FX_t + w_t \quad (2.17)$$

$$P_{t+1} = FP_tF^T + Q_t \quad (2.18)$$

where;

$$X_t = \begin{bmatrix} x \\ y \\ \dot{x} \\ \dot{y} \\ \ddot{x} \\ \ddot{y} \end{bmatrix}$$

$$F = \begin{bmatrix} 1 & 0 & t & 0 & \frac{t^2}{2} & 0 \\ 0 & 1 & 0 & t & 0 & \frac{t^2}{2} \\ 0 & 0 & 1 & 0 & t & 0 \\ 0 & 0 & 0 & 1 & 0 & t \\ 0 & 0 & 0 & 0 & 1 & 0 \\ 0 & 0 & 0 & 0 & 0 & 1 \end{bmatrix}$$

X_t is the state vector containing the position, velocity and acceleration parameters,

F is the state transition matrix,

w_t the process noise with zero mean and standard deviation σ_w ,

Q is the covariance matrix of the dynamic model driving noise vector, w_t

t is the sampling period and,

P_t is the state covariance matrix at time t .

The target measurement equation is given by Eq. 2.19.

$$Z_t = HX_t + v_t \quad (2.19)$$

where;

Z_t is the measurement vector which comprises only the position since in this study observation is made on the position vector only.

v_t is the measurement error with zero mean and standard deviation σ_v .

H is the measurement/ observation matrix given by;

$$H = \begin{bmatrix} 1 & 0 & 0 & 0 & 0 & 0 \\ 0 & 1 & 0 & 0 & 0 & 0 \end{bmatrix}$$

Correction step;

Eq. (2.20) is the Kalman filtering equation as it computes the updated estimate of the current state of the target and Eq. (2.21) is the updated estimate of the state covariance matrix.

$$\hat{X}_t = X_t + K_t y_t \tag{2.20}$$

$$\hat{P}_t = (I - K_t H) P_t \tag{2.21}$$

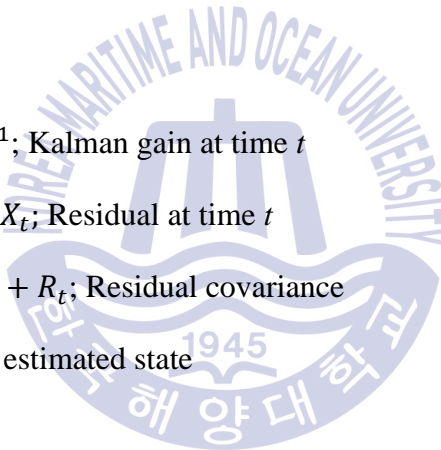
where;

$K_t = P_t H S_t^{-1}$; Kalman gain at time t

$y_t = Z_t - H X_t$; Residual at time t

$S_t = H P_t H^T + R_t$; Residual covariance

$\hat{\cdot}$ denotes the estimated state



Chapter 3. Simulation

3.1 Initial Input of Target Dynamics

The simulation tests were carried out on a warship moving at the initial relative speed of 50 m/s as observed from a stationary own ship. A sample signal of $n = 1,000$ data samples was investigated at sampling interval time of $t = 3\text{ s}$ which corresponds to the time of one aerial rotation of the radar antenna. The target's initial position as observed from the radar range measurements was $(573, 1038.4)$ after scan-conversion to produce Cartesian coordinates. Table 3.1 summarizes these initial set target states.

Table 3.1 Summary of the initial input target dynamics

| Position (x, y) | Relative speed (m/s) | Sampling interval (s) | Sample size (n) |
|--------------------|-------------------------|--------------------------|--------------------|
| 573, 1038.4 | 50.4 | 3 | 1,000 |

3.2 Input Motion Model of the Target Dynamics

The input model employed to generate the target dynamics is as shown in Eq. (3.1) for the horizontal motion and Eq. (3.2) for the vertical motion.

$$X_i = a[10\sin(1.2wi) + 7\cos(0.99wi) + 8\sin(0.7wi) + 6\cos(2wi) + 9\sin(3wi) + 5\cos(3wi)] + 10i ; \quad (3.1)$$

$$Y_i = b[20\cos(0.3wi) + 22\sin(2wi)]; \quad (3.2)$$

where; a and b are constants that serve to control the velocity of the input motion model.

From the set motion model described by Eqs. (3.1) & (3.2), the resulting signal was then sampled at intervals of three seconds to obtain the true trajectory of the target as shown in Fig. 3.1.

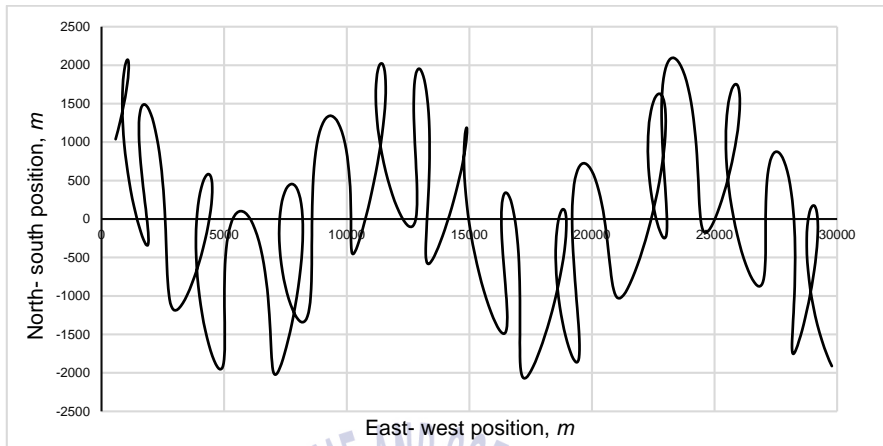


Fig. 3.1 Target's true trajectory

3.3 Noise Modelling

The observed position is the output obtained from the radar measurements and therefore includes an error. In this study, the noisy observation was obtained by corrupting the true state with zero mean random white Gaussian noise having a standard deviation, σ , of 10 m . Figs. 3.2 & 3.3 show the error distribution in the observation.

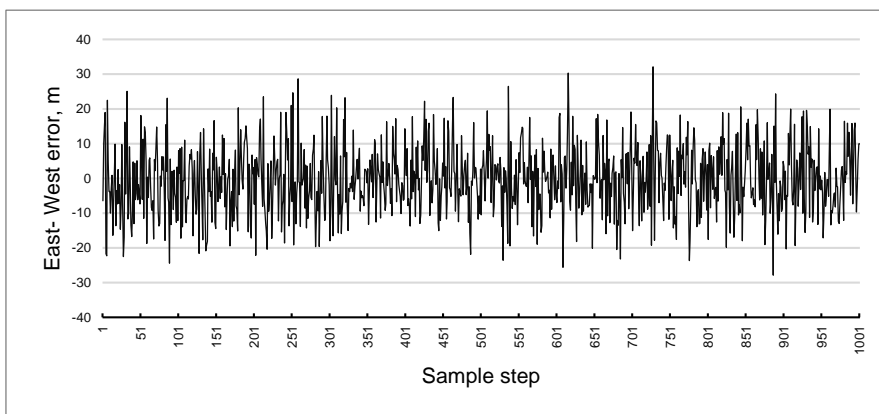


Fig 3.2 East-West error in the observation

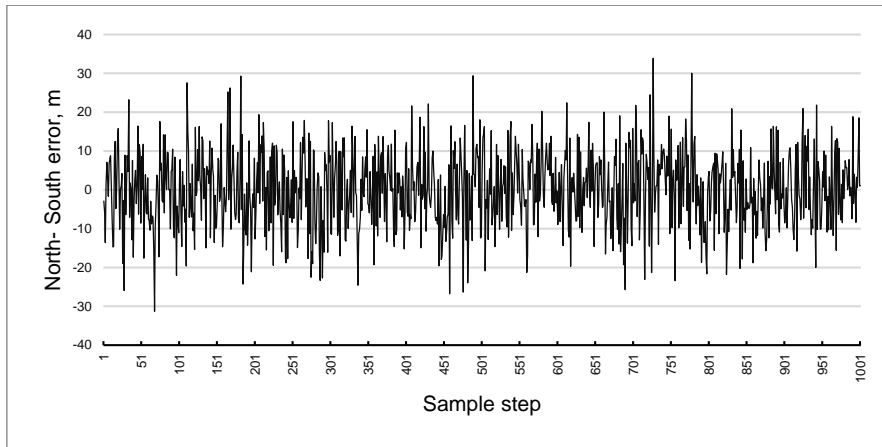


Fig. 3.3 North-South error in the observation

3.4. α - β - γ Filter Weight Selection and Computation

The selection and computation of the smoothing coefficients was based uniquely on the algorithm provided by the various filter design methods described in chapter 2. This sub-section explains how the filter weights were computed for each α - β - γ filter design model.

3.4.1 Filter gain coefficients selection using the Benedict-Bordner model

Since this design method does not provide an analytical solution for determining the position smoothing coefficient α , in this study, the position smoothing coefficient was determined experimentally through a trial and error method by plotting it against the corresponding innovation which is the total residual obtained from the difference between the observed position and predicted position trajectories as shown in Fig. 3.4. The interval evaluated was selected based on the stability constraints provided for by Jury (1964) for the α - β - γ tracking filter. The value of the α that best reduced the innovation was found to be $\alpha = 0.86$. Eqs. (2.7) & (2.8) were then used to compute the values of the velocity and acceleration smoothing coefficients as shown in Table 3.2.

Table 3.2 Smoothing coefficients obtained from Benedict-Bordner model

| α | β | γ |
|----------|---------|--------------------------|
| 0.8600 | 0.6488 | 4.4409×10^{-16} |

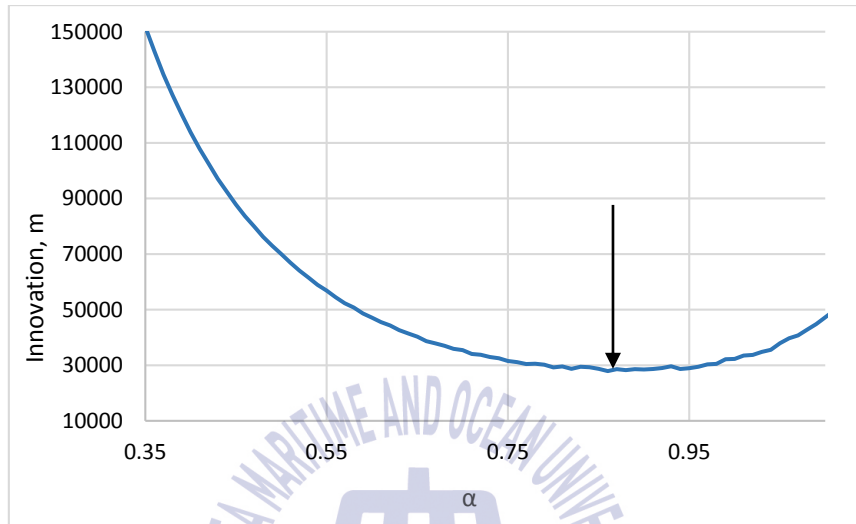


Fig. 3.4 Total residual between observed and predicted positions against corresponding value of position smoothing coefficient, α

3.4.2 Filter gain coefficients selection using the Gray-Murray model

The maneuverability and measurement noise variances were determined experimentally by an iterative trial and error method by changing the values of σ_w^2 and σ_v^2 error variances while simultaneously feeding the measurement data to the filter for each error variance. The output was then used to compute cumulative positional error which was then plotted against corresponding error variances. The purpose of this procedure was to identify the error variance coefficient corresponding to the least error. From the Figs. 3.5, 3.6, 3.7 and 3.8, the values of the maneuverability and measurement error variance coefficients corresponding to the minimum residual error are 10^{-3} and 1 respectively. Consequently the respective standard deviations are estimated to be $\sigma_w=0.03162$ and $\sigma_v=1$.

The tracking index was, therefore, computed as $\lambda=0.2846$ and, consequently the damping parameter, $r=0.6873$. The smoothing coefficients are then computed using Eqs. (2.11) ~ (2.13) and are obtained as displayed in Table 3.3.



Fig. 3.5 Cumulative error difference between observed and predicted positions against maneuverability error variance

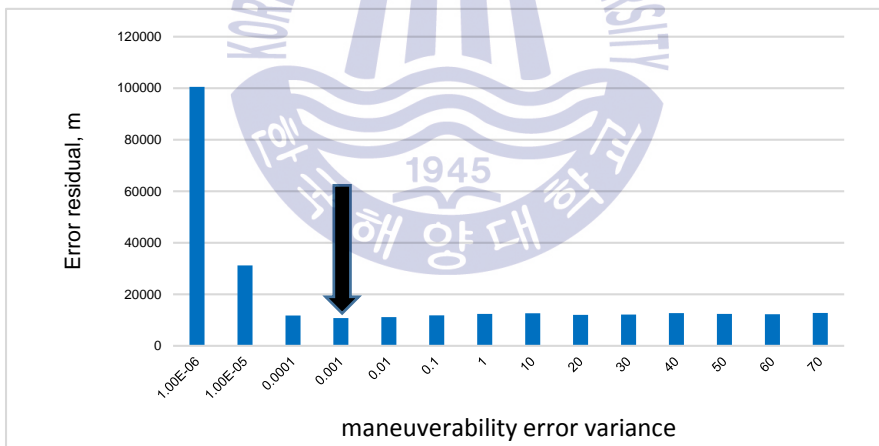


Fig. 3.6 Cumulative error difference between true and smoothed positions against maneuverability error variance

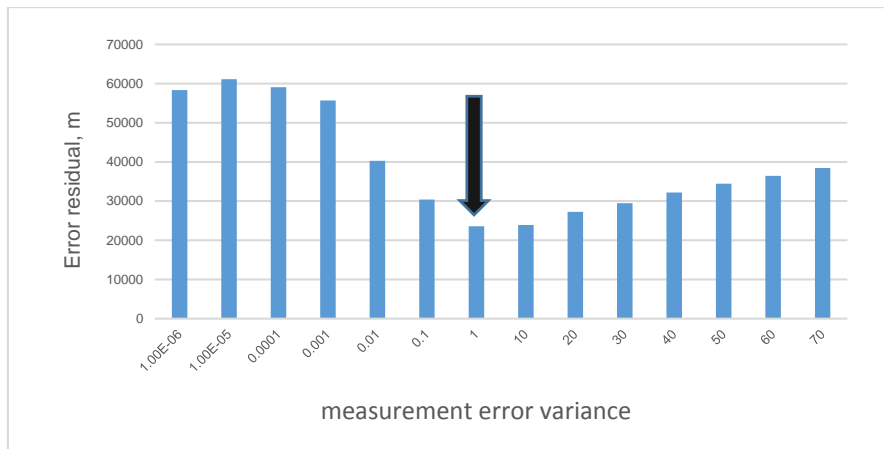


Fig.3.7 Cumulative error difference between observed and predicted positions against measurement error variance

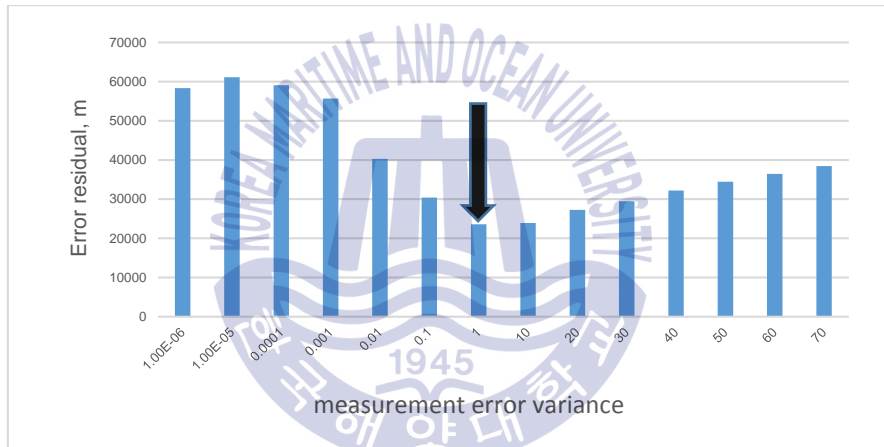


Fig. 3.8 Cumulative error difference between true and smoothed positions against measurement error variance

Table 3.3 Smoothing coefficients obtained from Gray-Murray model

| α | β | γ |
|----------|---------|----------|
| 0.5277 | 0.1956 | 0.0101 |

3.4.3 Filter gain coefficients selection using the fading memory model

It is known as the fading memory model since the filter weights depend on the value of the discounting factor such that a small damping parameter, ζ leads to a

short filter memory hence quickly discounting the older data causing little to no smoothing. On the contrary, a large ζ results in a longer filter memory causing heavy smoothing and a large dynamic lag. From Eqs. (2.13) ~ (2.15), the discounting factor, ζ is constrained to lie in the interval $[0, 1]$. Therefore, when $\zeta=0$, then $\alpha =1$ and from Eq. (2.4), the smoothed position and the observed position are superposed indicating that the filter has no memory hence no noise smoothing occurs. On the other hand, if $\zeta=1$, then $\alpha =0$ hence the predicted position and the smoothed position are superposed, a case of infinite memory thus heavy noise smoothing. An illustration of this is as shown in Figs. 3.9, 3.10 and 3.11. Figs. 3.9 and 3.10 represent cases of under- damping and over- damping respectively resulting in the large transient error, insensitivity to target maneuvers and filter instability as depicted in the trajectories. Fig. 3.11 represents a balance on the design specifications of the previous two figures demonstrating a better transient performance and an equally good stability in the output data as can be clearly seen in the stable output target trajectories that closely follow the desired signal.



Fig. 3.9 True, Observed, Predicted and Smoothed Position, Large Smoothing Coefficient ($\zeta=0.2$)

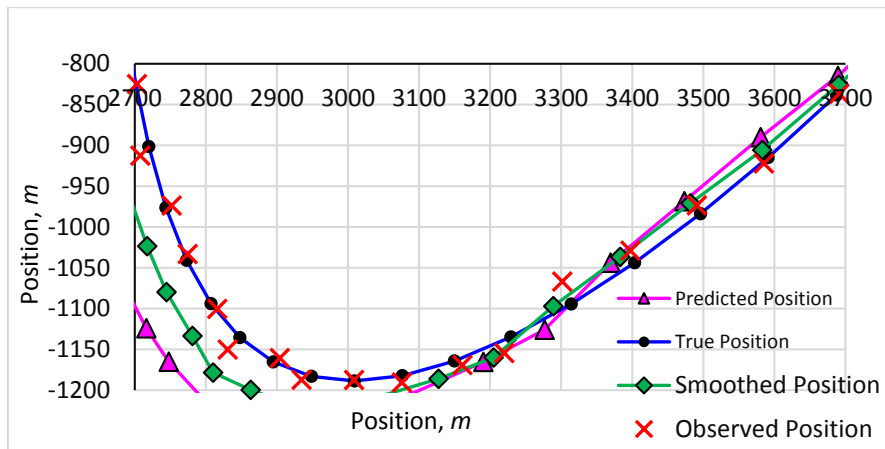


Fig. 3.10 True, Observed, Predicted and Smoothed Position, Small Smoothing Coefficient ($\zeta=0.8$)

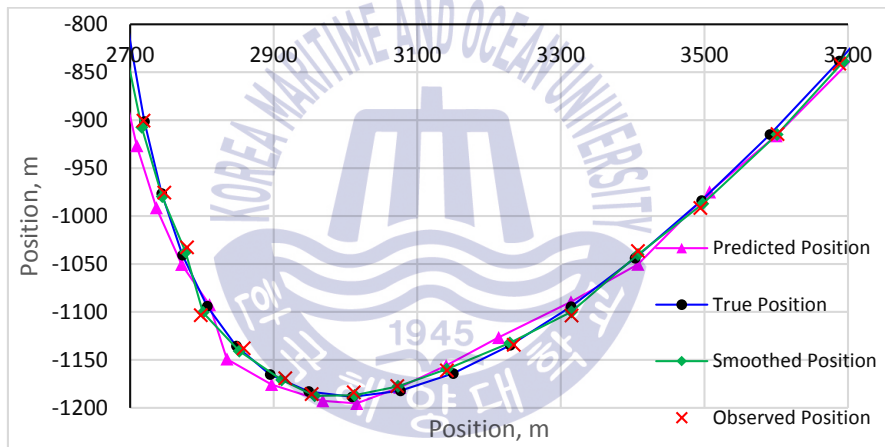


Fig. 3.11 True, Observed, Predicted and Smoothed Position, Optimal Smoothing Coefficient ($\zeta=0.64$)

3.4.3.1 Fading memory model optimization

This design method relates the smoothing coefficients α , β and γ with a discounting factor, ζ consequently making the filter weights values dependent on the value of ζ . Therefore, in order to obtain the optimal smoothing coefficients, the ζ is adjusted experimentally through trial and error until the best value that leads to the best performance is arrived at. Two optimization approaches are

investigated in this study, that is, optimization by target's position and optimization by target's velocity and acceleration.

3.4.3.1.1 Optimization by position

This method involves comparing the true position, obtained from plotting Eqs. (3.1) and Eqs. (3.2), with the predicted position and smoothed position, and computing the RTP (residual between the True and Predicted Position) and RTS (residual between the True and Smoothed Position) then plotting the total positional error against a range of the discounting factor, ξ . The value of ξ corresponding to the least residual error is considered the optimal ξ and hence results in the optimal smoothing coefficients.

Fig. 3.12 shows the positional trajectories depicting the true, observed, predicted and smoothed positions tracks. The curve enclosed in the rectangle is enlarged for clear viewing as shown in Fig. 3.13 and lies in the interval [2700, 3700] in the x- axis coordinate. Fig. 3.14 and 3.15 are the residual errors obtained from the difference between the true and predicted, and true and smoothed positions respectively corresponding to Fig. 3.12. In this case the damping parameter, ξ was selected arbitrarily as 0.5 for illustration purpose of the optimization procedure.

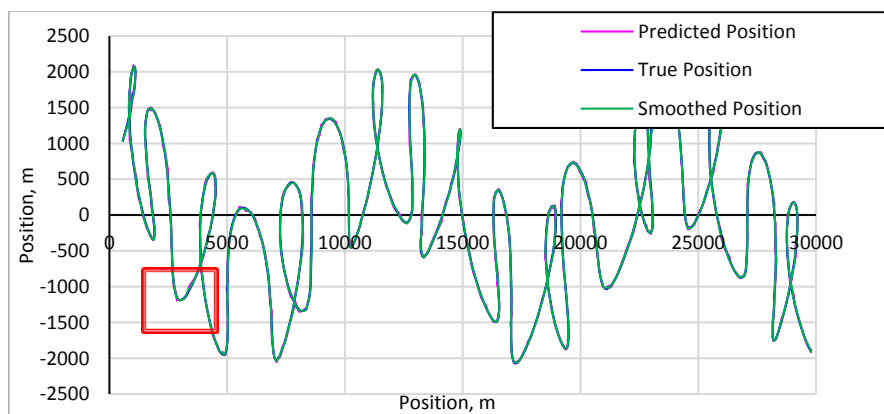


Fig. 3.12 Target's True, Observed, Predicted and Smoothed Position ($\xi=0.5$)

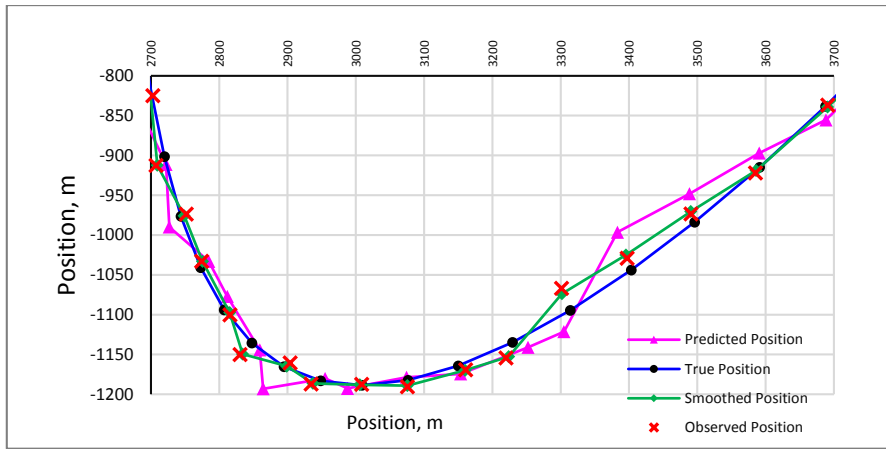


Fig. 3.13 Enlarged View of target's True, Observed, Predicted and Smoothed Position ($\xi=0.5$) corresponding to Fig. 3.12

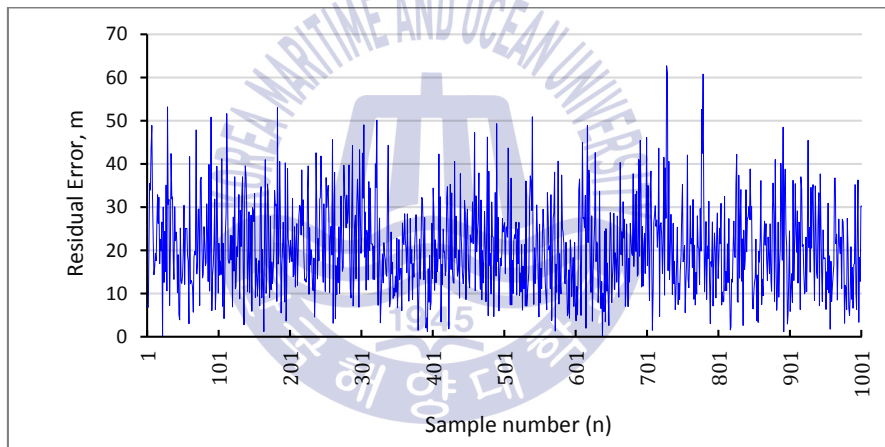


Fig. 3.14 Difference between the true and predicted positions corresponding to Fig. 3.12

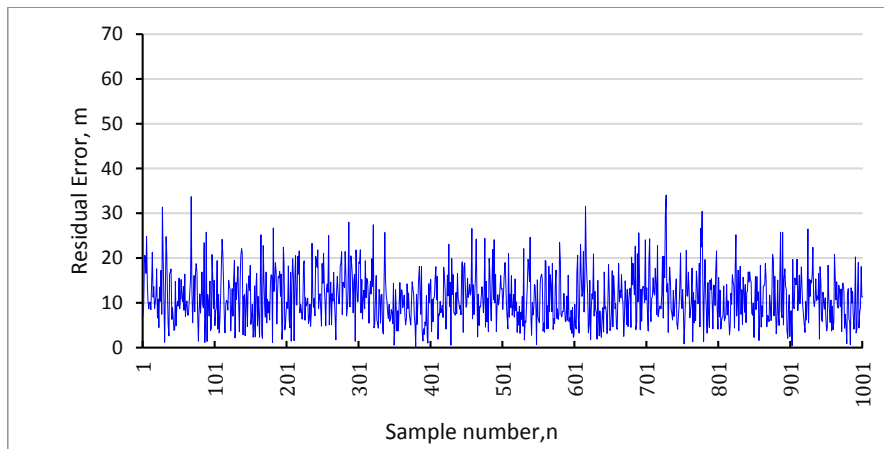


Fig. 3.15 Difference between the true and smoothed positions corresponding to Fig. 3.12

Optimization criteria of the filter was based on reduction of residual error to a minimum. In this case, residual error is the distance between two measurements at the same point in time. For example the residual error T-P indicates the distance between the true position and predicted position at time t . Fig. 3.14 shows the residual error T-P obtained for $\zeta=0.5$, and the summation of residual error is the total error obtained from the whole sample frame over the given tracking duration. To determine the optimal discounting factor, ζ is set to lie in the interval 0 to 0.8 with a step size of 0.01. It was found that values of ζ exceeding 0.8 resulted in a sharp increase of the residual error. This can be attributed to over-damping resulting in large dynamic lag. Fig. 3.16 shows the summation of residual error T-P corresponding to varying values of the discounting factor, ζ .

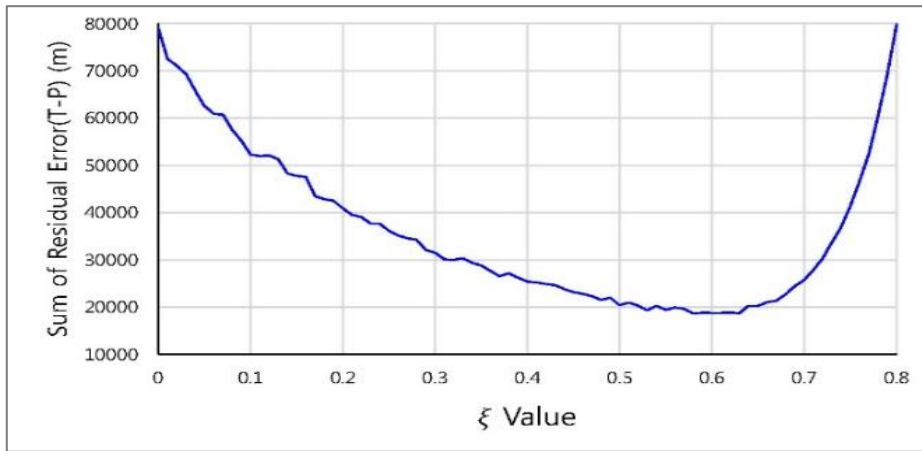


Fig. 3.16 summation of residual error T-P for varying ksi

The variations along the trajectory on Fig. 3.16 are as a result of addition of noise to the observation. In order to obtain a smooth curve the simulation is carried out thirty times. Fig. 3.17 shows the superposed curves of thirty simulation runs for the summation of residual error $T-P$. From this, the value of average error summation for each ξ can be computed and consequently Fig. 3.18 is obtained. It can be clearly seen that when $\xi=0.62$, the summation of residual error has a minimum point which implies that 0.62 is the optimal ξ determined by the method of evaluation by summation of residual error of true and predicted position.

Similarly, when evaluation is done using the summation of residual error $T-S$ (true and Smoothed position), the optimal discounting factor is obtained as shown in Fig. 3.19. The results show that the optimal discounting factor is, $\zeta=0.64$.

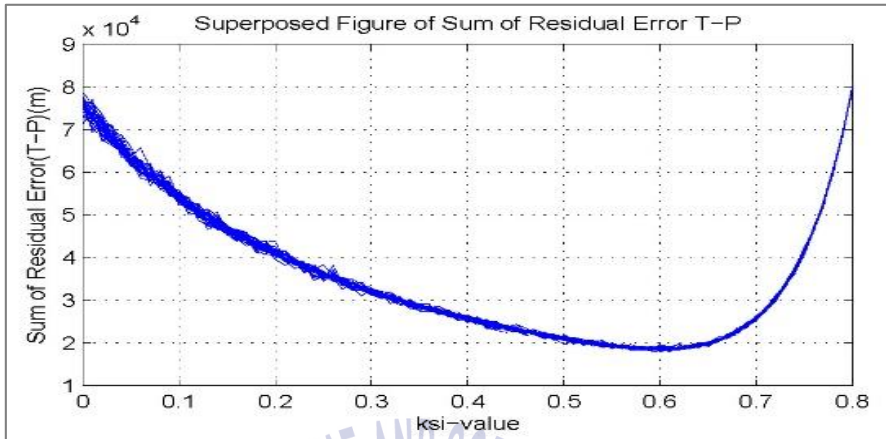


Fig. 3.17 Summation of the error difference between true and predicted positions for varying values of ζ after thirty simulation runs

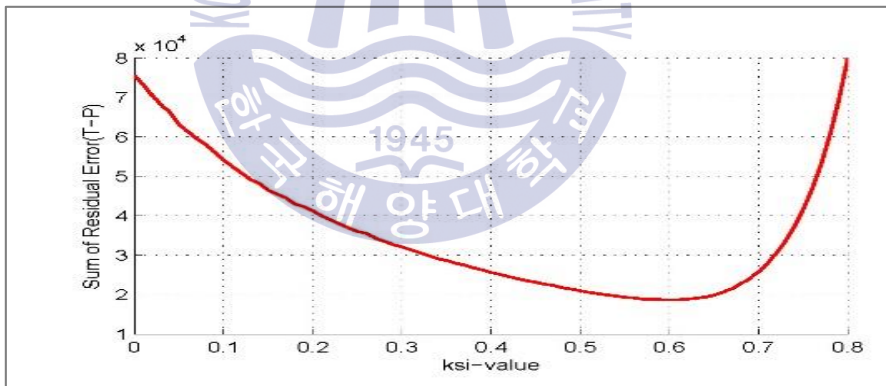


Fig. 3.18 Summation of the error difference between true and predicted positions for average values of summation for each ζ corresponding to Fig. 3.16

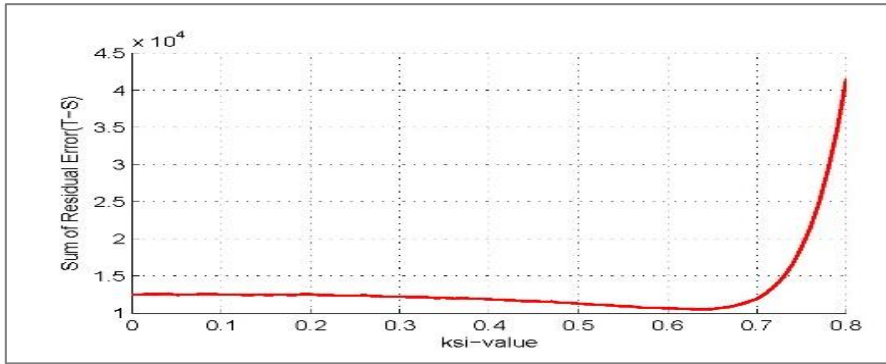


Fig. 3.19 Summation of the error difference between true and Smoothed Positions for average values of ζ after 30 Simulation runs

3.4.3.1.2 Optimization by velocity and acceleration

The smoothed velocity and acceleration are obtained after filtering as shown in Eqs. (2.5) & (2.6) in chapter 2. The first and second derivatives were obtained from Eqs. (3.1) & (3.2) resulting in the true (desired) target's velocity and acceleration as shown in Eqs. (3.3) & (3.4) respectively. Since the closer to the true state variables the smoothed variables are the better the performance, this method employs the residual error of true and smoothed velocity, and the residual error of true and smoothed acceleration to determine the optimal ζ .

$$\frac{dX_i}{dt} = a[12w\cos(1.2wi) - 6.93w\sin(0.99wi) + 5.6w\cos(0.7wi) - 12w\sin(2wi) + 27w - 15w\sin(3wi)] + 10 \quad (3.3)$$

$$\frac{dY_i}{dt} = b[-6w\sin(0.3wi) + 44w\cos(2wi)]$$

$$\frac{d^2X_i}{dt^2} = a[-14.4w^2\sin(1.2wi) - 6.8607w^2\cos(0.99wi) - 3.92w^2\sin(0.7wi) - 24w^2\cos(2wi) - 81w^2\sin(3wi) - 45w^2\cos(3wi)] \quad (3.4)$$

$$\frac{d^2Y_i}{dt^2} = b[-1.8w^2\cos(0.3wi) - 88w\sin(2wi)]$$

After running thirty simulations and calculating the average summation of residual error corresponding to each ζ , Fig. 3.19 and Fig. 3.20 were obtained. The minimum point on the curve indicates that optimal ζ is 0.56 on evaluation using residual resulting from true and smoothed velocity difference. On the other hand, on evaluation by the residual obtained from difference between the true acceleration and smoothed acceleration, the optimal ζ is 0.62 as indicated in Fig. 3.20.



Fig. 3.20 Average cumulative error between true and smoothed velocity for each value of ζ after thirty simulation runs

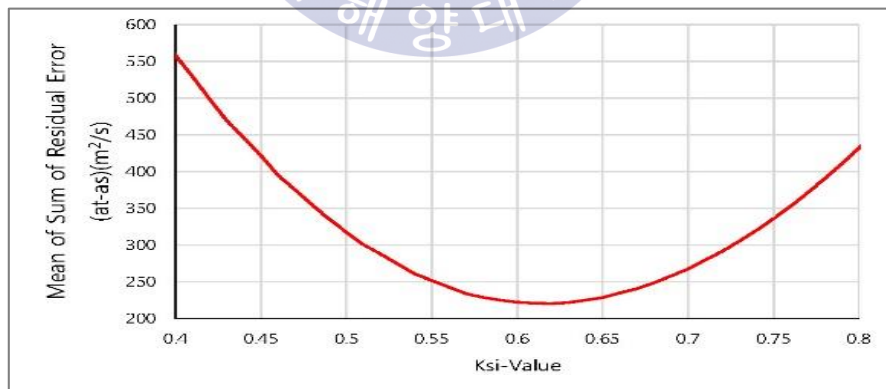


Fig. 3.21 Average cumulative error between true and smoothed acceleration for each value of ζ after thirty simulation runs

From the above analysis, the initial velocity and the average velocity is a constant value, and the optimal ζ is close to 0.6. From the position Eqs. (3.1) & (3.2), if the constants a, b are varied, the initial velocity and average velocity also changes.

Table 3.4 shows the optimal discounting factor obtained for various initial and average target velocities. The quantities a, b serve to control the numerical size of the initial and average target velocity. The results indicate that different relative speeds result in different optimal filtering coefficients. A target model moving at very high initial relative speed requires a low value of the optimal damping parameter compared to a slower target.

Table 3.4 Optimal ζ for various initial velocities

| A | b | Initial velocity (m/s) | Average velocity (m/s) | OKRTPP | OKRTSP | OKRTSV | OKRTSA |
|----|-----|------------------------|------------------------|--------|--------|--------|--------|
| 3 | 5 | 12.9 | 10.34 | 0.77 | 0.78 | 0.75 | 0.78 |
| 15 | 30 | 31.30 | 19.24 | 0.65 | 0.68 | 0.62 | 0.67 |
| 30 | 50 | 50.36 | 30.33 | 0.60 | 0.64 | 0.56 | 0.62 |
| 60 | 90 | 88.43 | 54.02 | 0.53 | 0.57 | 0.49 | 0.55 |
| 70 | 120 | 111.40 | 69.28 | 0.52 | 0.55 | 0.45 | 0.53 |
| 90 | 160 | 145.40 | 91.20 | 0.50 | 0.54 | 0.43 | 0.51 |

where;

OKRTPP: Optimal ζ evaluated by summation of the residual computed from the difference between the true position and predicted position;

OKRTSP: Optimal ζ obtained from summation of the residual resulting from difference between the true position and smoothed position;

OKRTSV: Optimal ζ evaluated by summation of the residual error between the true velocity and smoothed velocity and,

OKRTSA: Optimal ξ evaluated by summation of the residual error between the true acceleration and smoothed acceleration.

Table 3.5 shows a summary of the smoothing constants as obtained from the fading memory design method as computed using Eqs. (2.14)~ (2.16) as discussed in section 2.

Table 3.5 Smoothing coefficients obtained from fading memory model

| α | β | γ |
|----------|---------|----------|
| 0.5277 | 0.1956 | 0.0101 |

3.5 Kalman Filter Tuning

Tuning the Kalman filter involves a careful process of estimation of the process noise covariance and the measurement noise covariance which in turn increases the sensitivity of the filter which produces near optimal estimates of the required target dynamics. Since the effects of both R and Q are negatively correlated, owing to the fact that they occur in the measurement and state equation respectively, the matrices need to be carefully selected and tuned to avoid divergence of the filter estimates rendering them useless. In addition, given that the R and Q matrix in this study are a fixed value throughout the filtering process, the initial choice of both covariance matrices is crucial in ensuring a good and stable performance of the filter.

3.5.2 Q Covariance Matrix Tuning

The matrix Q in the Kalman filter reflects the uncertainty in the target's trajectory during maneuvers and therefore it is the process or dynamic noise w covariance matrix with a variance, σ_w^2 . The tuning process in this study was achieved based on a procedure paralleling that employed in the Gray-Murray

model for determination of the measurement and maneuverability error variance. It involved changing the covariance matrices alternately. For instance, in order to obtain the Q covariance matrix, the measurement noise covariance matrix R , was held constant as measurement data was simultaneously fed to the filter while constantly changing the Q matrix coefficient for each simulation run. The output was then used to compute cumulative positional error which was then plotted against corresponding Q covariance matrix coefficients. The Q covariance matrix coefficient corresponding to the least error was then obtained. From the Figs. 3.22 and 3.23, the value of Q covariance matrix coefficient corresponding to the minimum residual error is 10^{-3} . The process noise covariance matrix Q obtained from this process is as represented by the Eq. (3.5).

$$Q = 10^{-3} \begin{bmatrix} 1 & 0 & 0 & 0 & 0 & 0 \\ 0 & 1 & 0 & 0 & 0 & 0 \\ 0 & 0 & 1 & 0 & 0 & 0 \\ 0 & 0 & 0 & 1 & 0 & 0 \\ 0 & 0 & 0 & 0 & 1 & 0 \\ 0 & 0 & 0 & 0 & 0 & 1 \end{bmatrix} \quad (3.5)$$

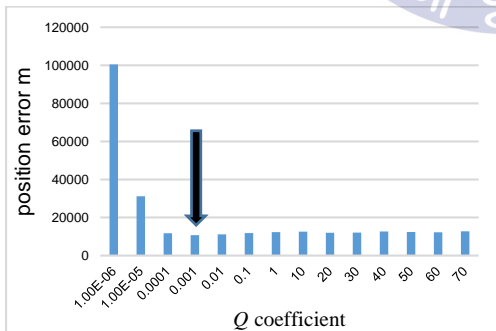


Fig. 3.22 Cumulative error difference between observed and predicted positions against Q matrix coefficient

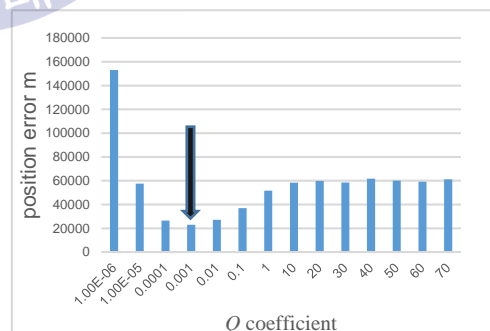


Fig. 3.23 Cumulative error difference between true and smoothed positions against Q matrix coefficient

3.5.2 R Covariance Matrix Tuning

The R matrix shows the accuracy of the radar measurement. Hence, it is the covariance matrix of the measurement error v , with a variance of σ_v^2 . The tuning process of the R covariance matrix is similar to the one described in sub-section 3.5.1 for determination of the maneuverability error covariance matrix coefficient. Hence, to determine the R covariance matrix, the Q covariance matrix was held constant while feeding the measurement data to the filter simultaneously as the measurement noise covariance matrix is altered with every simulation run. The output was then used to compute cumulative positional error which was then plotted against corresponding measurement noise covariance matrix coefficients. The covariance matrix coefficient corresponding to the least error was then obtained as the value of the optimal measurement noise covariance coefficient. From the Figs. 3.24 and 3.25, the value of R covariance matrix coefficient corresponding to the minimum residual error is 1 and is represented by the matrix shown in Eq. (3.6).

$$R = \begin{bmatrix} 1 & 0 \\ 0 & 1 \end{bmatrix} \quad (3.6)$$

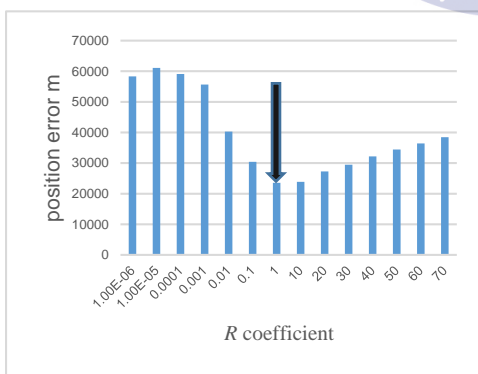


Fig. 3.24 Cumulative error difference between observed and predicted positions against R matrix coefficient

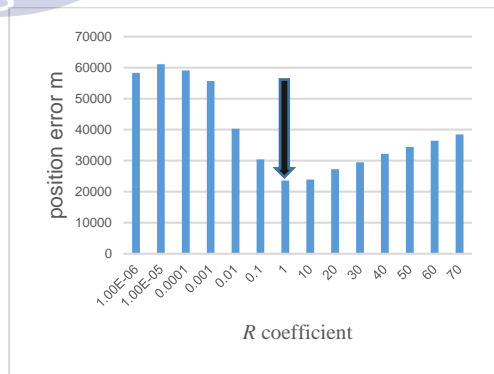


Fig. 3.25 Cumulative error difference between true and smoothed positions against R matrix coefficient

3.6 Results Analysis and Discussion

In this study, the comparison of the filters was based on three performance indices, that is, tracking and estimation error reduction, sensitivity of the filter to target maneuvers and output data stability, and variance reduction ratio (VRR).

Filter's capability to minimize the tracking and estimation noise levels was achieved by comparing the size of the error in the estimated and predicted positions that is, estimation and prediction error determination respectively as a measure of the error reduction capability of the filter. Estimation error is obtained by computing the deviation of the estimated data from the true position for each sample. Similarly, prediction error indicates how far the predicted position deviates from the true position hence it is the tracking error. Sensitivity of the filter to target maneuvers and data stability was indicated by the filter's ability to follow the target steadily and without divergence of the data samples which could lead to loss of target and was determined by observation of the state of stability and steadiness of the trajectories obtained using the different filtering design methods considered in this study. Of importance was to observe how closely the filter follows the true target trajectory which is the desired output. And finally, the variance reduction ratio was evaluated using the Eqs. (1.1) ~ (1.3) which indicates the measurement noise reduction for position, velocity and acceleration.

3.6.2 α - β - γ Filter Results and Remarks

Figs. 3.26, 3.27 & 3.28 show the true, observed, predicted and smoothed positions trajectories obtained from the tracking problem using the various α - β - γ filter models under consideration in this study. The figures represent the positional trajectories for the Benedict-Bordner filter, Gray-Murray model, the fading memory filter model respectively. Of the three models under investigation, the Gray-Murray model appears to follow the target quite well with high sensitivity to changes in target maneuvers as indicated by the stability and steadiness of the

trajectories as the target transitions from one point to the next. In addition, the output trajectories that is, the predicted and smoothed position trajectories can be observed to transition very smoothly and closely to the true trajectory for the entire duration of the tracking period. The fading memory model performs nearly as well as the Gray-Murray model except for a few fluctuations of data samples at several points along the target's curves which indicate a reduced sensitivity at these points on the targets' trajectories as the target maneuvers. As for the Benedict-Bordner model, shown in Fig. 3.26, the filter performs worst, based on sensitivity to target maneuvers and data stability, compared to the other two α - β - γ filters as indicated by the visibly clear jerky motion at the beginning of the tracking process. However, as tracking continues the trajectories stabilize and the tracking accuracy can be seen to also increase.

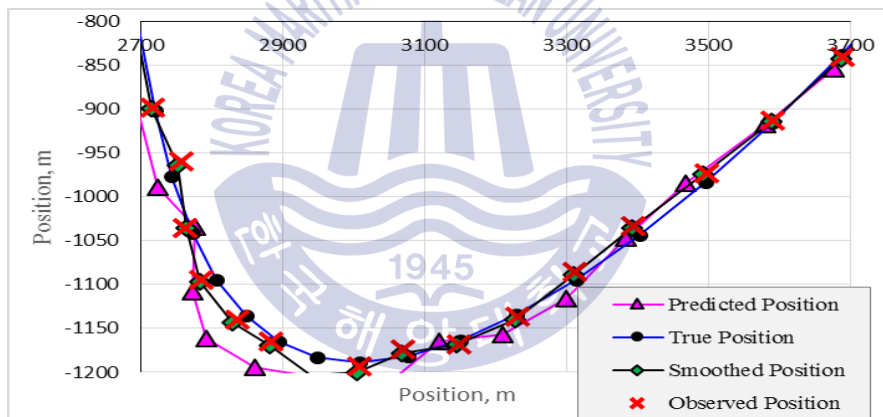


Fig. 3.26 Target's True, Observed, Predicted and Smoothed Position, *Benedict-Bordner model*

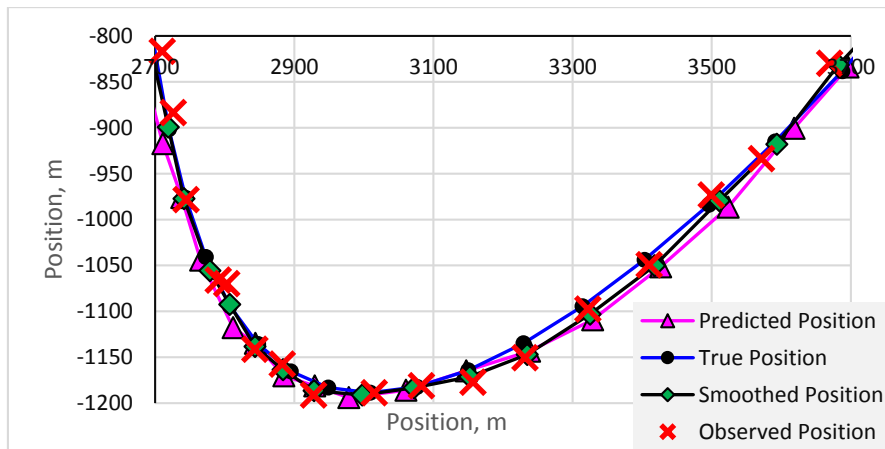


Fig. 3.27 Target's True, Observed, Predicted and Smoothed Position, *Gray-Murray model*

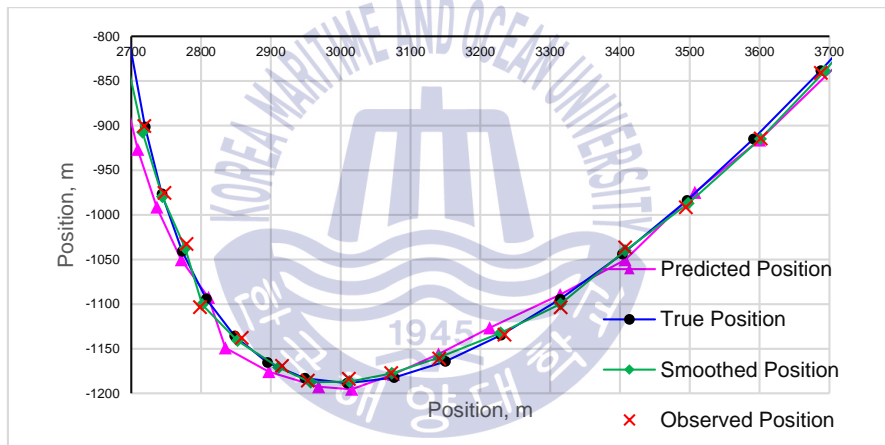


Fig. 3.28 Target's True, Observed, Predicted and Smoothed Position *fading memory model, ($\xi=0.64$)*

Figs. 3.29, 3.30 & 3.31 show the total prediction (tracking) errors resulting from Benedict-Bordner model, the Gray-Murray model and the fading memory filter model respectively. Figs. 3.32, 3.33 & 3.34 are the total estimation errors obtained from the Benedict-Bordner model, the Gray-Murray model and the fading memory filter model respectively.

These results show that the fading memory model has the highest accuracy in both tracking and estimation of the position of the target warship among the other α - β - γ filters as can be seen from the small error values obtained, followed by the Gray-Murray filter model. The Benedict-Bordner filter performs the worst in terms of tracking and estimation noise reduction for both prediction and estimation as indicated by the resulting big errors values. This can be explained by the fact that the design of this filter is based on the requirement for satisfying a good transient response. And since performance of a filter is a tradeoff between a good transient response and noise reduction, the filter then performs badly when applied to meet the requirement for tracking error reduction.

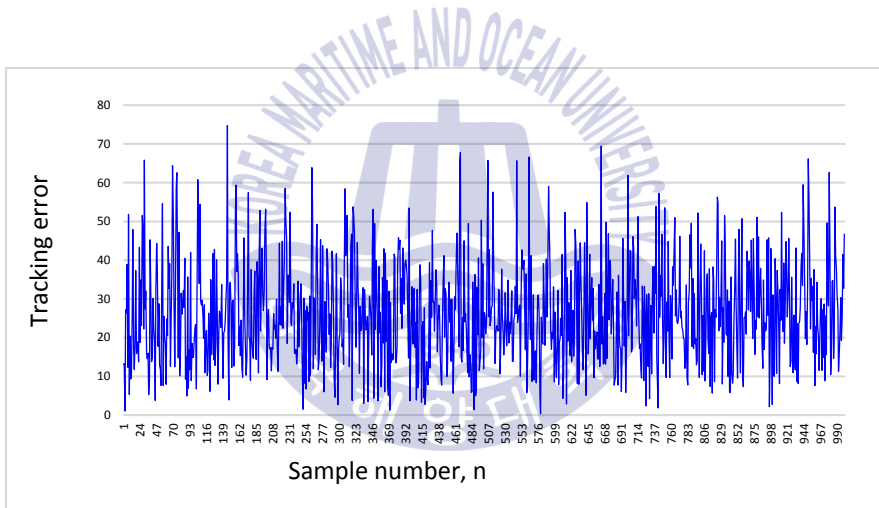


Fig. 3.29 Total prediction error, *Benedict- Bordner model*,
error= 26, 326 m

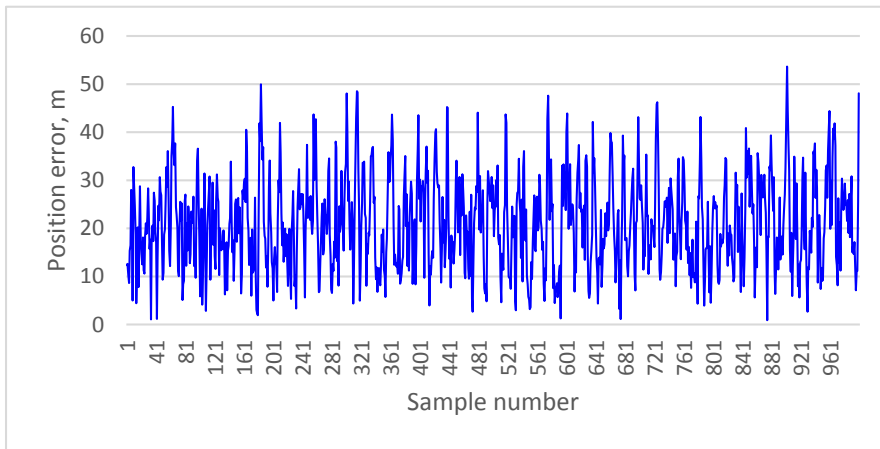


Fig. 3.30 Total prediction error, *Gray-Murray model*,
error= 21071 m

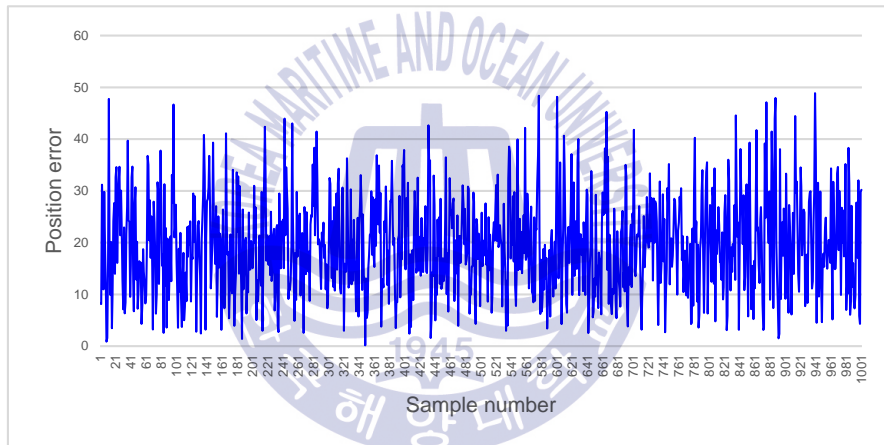


Fig. 3.31 Total prediction error, *fading memory model*,
error= 19, 622 m

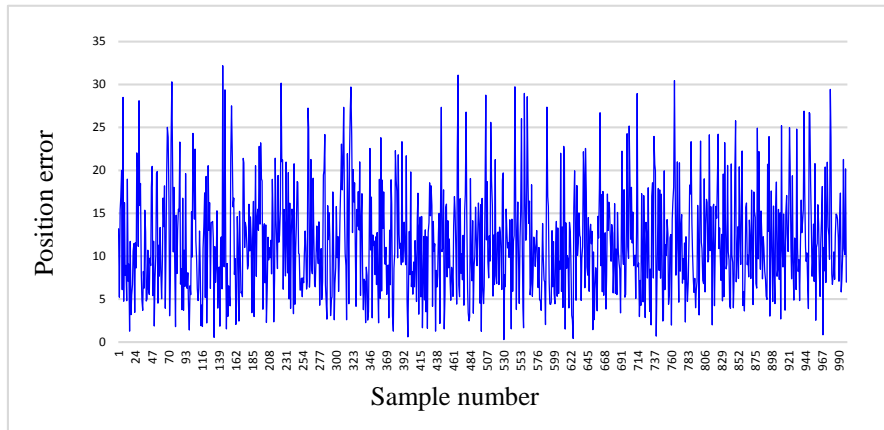


Fig. 3.32 Total estimation error, *Benedict-Bordner model*,
error= 11, 677m

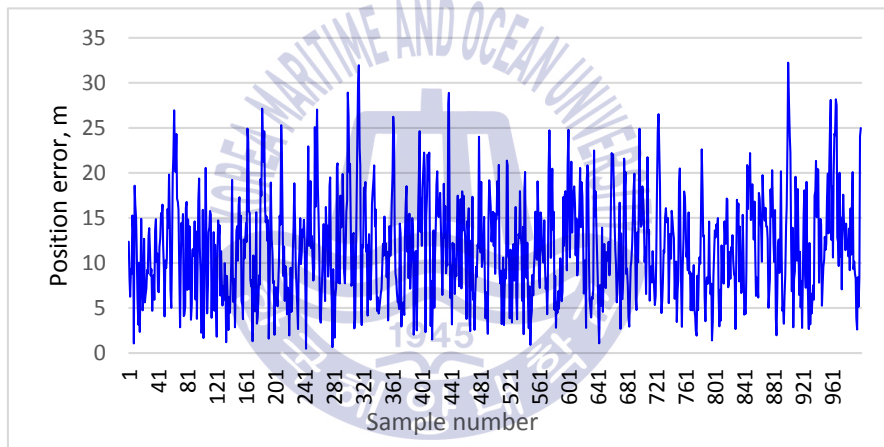


Fig. 3.33 Total estimation error, *Gray-Murray model*,
error= 11, 693 m

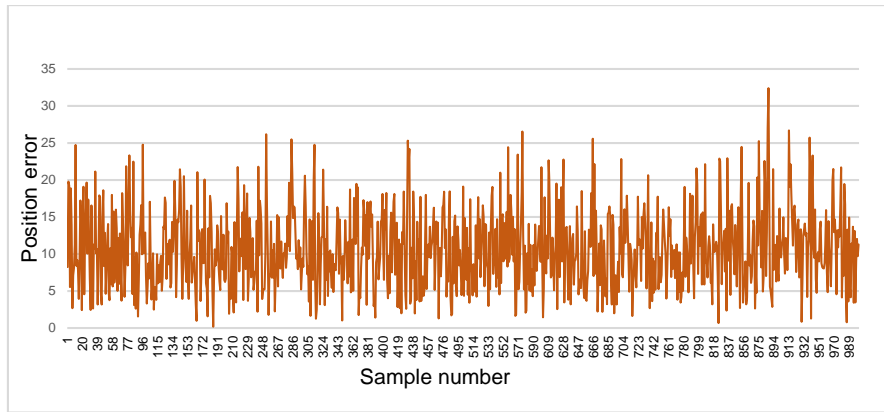


Fig. 3.34 Cumulative estimation error, *fading memory model*,
error = 10653 m

Using Eqs. (1.1) ~ (1.3) and the smoothing coefficients values as obtained from different filter models, the variance reduction ratios (VRRs) for each of the α - β - γ filter model investigated were computed and recorded as displayed on Table 3.6. From the results, the Gray-Murray model out-performs the other two filters as indicated by the small values obtained for both position and velocity variance reduction ratios in reducing the measurement noise. This is followed by the fading memory model and finally the Benedict-Bordner model. In this study, the acceleration variance reduction is of little consequence as the filter design is essentially for tracking nearly constant acceleration. Thus, the acceleration of the target does not affect the system dynamics much and hence the reason for the extremely small values of VRR resulting from the determination of the acceleration variance reduction ratios.

Table 3.6 Variance Reduction Ratios

| Filter type | Position VRR | Velocity VRR | Acceleration VRR |
|---------------------|--------------|--------------|--------------------------|
| Gray-Murray | 0.4743 | 0.0061 | 1.8711×10^{-06} |
| Fading memory model | 0.7172 | 0.0142 | 3.7829×10^{-05} |
| Benedict-Bordner | 0.7862 | 0.0667 | 3.4712×10^{-33} |

3.6.2 Kalman Filter Results and Remarks

With regard to sensitivity to target maneuvers and data stability, the Kalman filter was defined by prediction and estimation trajectories marred with erratic changes and fluctuations at various points on the trajectories, indicating data instability, throughout the tracking duration an indication of the filter's inability to respond efficiently to maneuvers particularly for this type of target motion dynamics. The results are as shown in Fig. 3.35.

Based on tracking and estimation error reduction, the results of the Kalman filter are as shown in Figs 3.36 & 3.37. The filter outperforms all the other three filters discussed in sub- section 2 above as it possesses the best accuracy as indicated by the small values of both the tracking and estimation errors obtained. These results indicate that the Kalman filter is an efficient estimator, but not suitable for following a highly maneuvering target.

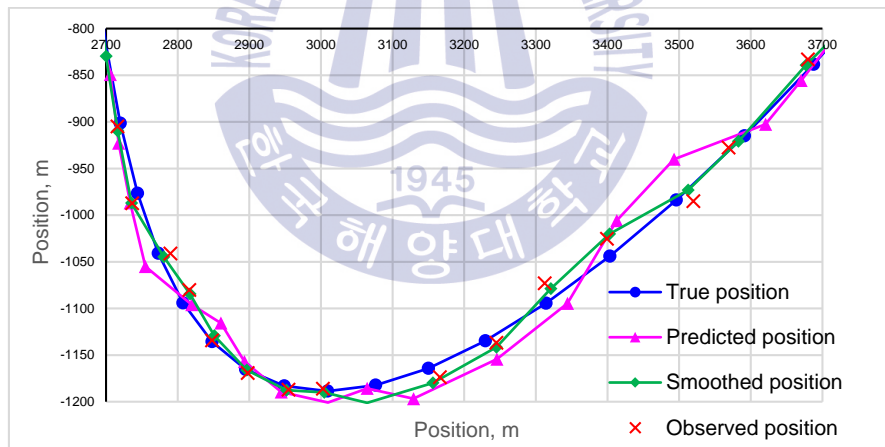


Fig. 3.35 Target's True, Observed, Predicted and smoothed Position, *Kalman Filter*

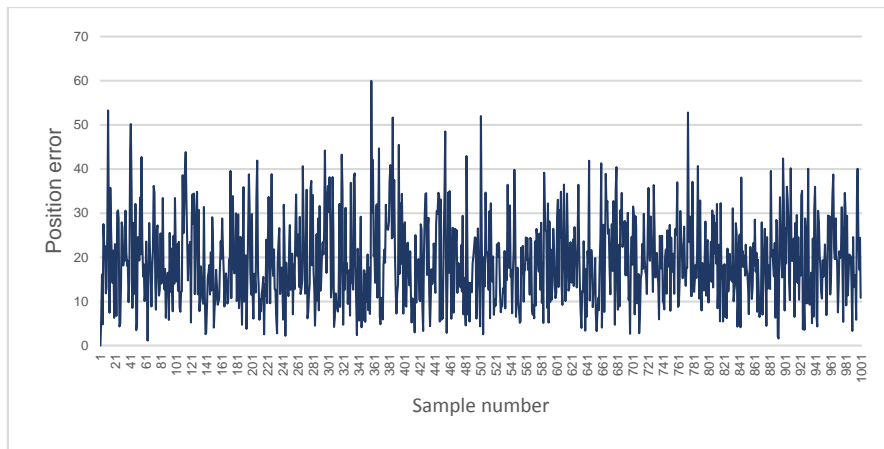


Fig.3.36 Total prediction error, *Kalman filter*, error=19,104 m

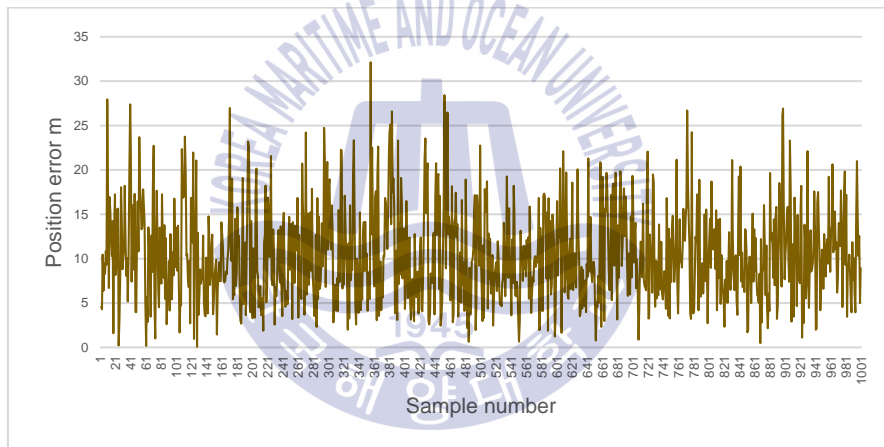


Fig. 3.37 Total estimation error, *Kalman filter*, Error=10,492 m

3.6.3 Kalman Filter vs. α - β - γ Filter

Overall, on the basis of sensitivity to target maneuvers and data stability, the α - β - γ filters out-performed the Kalman filter which was clearly defined by overshootings and fluctuations at various points on the output trajectories. This can be explained by the fact that the Kalman filter is not designed to handle maneuvering targets hence the unsteady output trajectories. It however minimizes the tracking

and estimation error better compared to α - β - γ filters as depicted by the small error values obtained. Nevertheless, the difference in error between the Kalman filter and the fading memory model is only slight as shown in Table 3.7 which provides a brief summary of a quick overview of the numerical values of the errors placed side by side for easier comparison at a glance.

Table 3.7 Summary of the tracking and estimation accuracy

| Filter type | | Tracking error (m) | Estimation error (m) |
|--------------------------------------|------------------------|--------------------|----------------------|
| α - β - γ filter | Benedict-Bordner model | 26,326 | 11,677 |
| | Gray-Murray model | 21,071 | 11,693 |
| | Fading Memory model | 19,622 | 10,653 |
| Kalman filter | | 19,104 | 10,492 |



Chapter 4 Conclusion and Future Prospects

In any research invested in the study and analysis of tracking filters, the most crucial objective is to attain a filter that meets the requirements for a particular application. Therefore, in selecting a particular filter the performance analysis comes in handy in order to select the best filter design that satisfies the design specifications.

In this study, four tracking filters, that is the Kalman filter, Benedict-Bordner constant acceleration filter model, Gray-Murray model and the fading memory α - β - γ filter model have been investigated for comparison based on their performance. The performance criteria involves determination of the filter's ability to reduce tracking and estimation noise, sensitivity to changes in target's tracks and data stability while tracking a highly maneuvering target with a random white gaussian error input, and determination of variance reduction ratio for each α - β - γ filter. The filters' capability to reduce tracking and estimation noise was a function of the residual error in the prediction and estimation data, and was computed by determining the deviation from the true trajectory of the predicted and smoothed trajectories respectively. Sensitivity to target maneuvers and data stability was determined through observation of the steadiness and stability of the target trajectories while, the variance reduction ratios were determined from analytically derived equations. Simulation tests were carried out under similar initial conditions of set target's input motion model on each filter.

Prior to performance comparison, the Fading memory model was optimized based on total residual error reduction achieved by adjusting the discounting factor in order to obtain the ζ that reduced the residual error the most. Optimization results showed that the optimal ζ is dependent on the speed of the target under consideration. In other words, different targets undergoing disparate

motion dynamics would have varying optimal gain parameters. For the target motion dynamics tested in this study, the optimal ζ was found to be equivalent to 0.62. This value was then used in computing the gains of the filter.

Simulation results demonstrated that based on the ability to follow the maneuvering target with sensitivity and data stability, the Benedict-Bordner model depicted an unstable motion marred with fluctuations and overshooting tendencies along the output trajectories at the beginning of the tracking duration. As plotting progressed, however, the trajectories seemed to stabilize and a closer look even showed increased accuracy. The Kalman filter was also characterized by variations along its trajectories implying its insensitivity in following this type of target motion as the fluctuations were spread across the entire lengths of the output trajectories which consequently indicated data instability. The Gray-Murray model, on the other hand, depicted quite a high order of sensitivity to target maneuvers and data stability which was visible from the obtained smooth curves of the output position trajectories indicating a higher efficiency in following the highly maneuvering target than the fading memory model which had a few variations at different points of the trajectories.

In terms of tracking and estimation noise reduction, the Kalman filter had a higher accuracy in both prediction and estimation of the target's position as compared to the optimal α - β - γ filters as demonstrated by the small error values obtained using the Kalman filter. The Benedict-Bordner model showed the worst ability to reduce noise as can be seen from the large deviations from the true trajectory obtained in the tracker for both prediction and estimation states. This is perhaps due to the fact that this filter is designed to essentially accentuate the transient response and, since performance of a filter is a tradeoff between a good transient response and error reduction, the filter then performs badly as tracking error minimizer. The fading memory model out-performed the other two α - β - γ

filters in this respect of tracking and estimation error reduction followed by the Gray-Murray model.

The results obtained from computation of the variance reduction ratio indicated that the Gray-Murray model out-performed the other two α - β - γ filters as it had the smallest values followed by the fading memory model. The variance reduction was a measure of the measurement noise reduction. It was also noted that the acceleration of the target had no effect on the system dynamics, hence the reason for the extremely small values of VRR resulting from the determination of the acceleration variance reduction ratios.

Overall, the critically damped filter not only depicted its efficiency in following the highly maneuvering target and possessing a good tracking noise reduction capability, but also its design simplicity and low computational load made it easy to implement.

Future study will involve tracking the high dynamic target warship while own ship is also on motion. In addition, a further improvement of the critically damped filter would be to use the jerky model filter in order to enhance the sensitivity to changes in tracks by the target during maneuvers and especially at points of sudden changes in speed and course along the target trajectory.

Reference

- [1] Benedict T. R. and Bordner G. W. (1962). "Synthesis of an Optimal Set of Radar Track-While-Scan Smoothing Equations," IRE Trans. on Automatic Control, AC-7, pp.27-32.
- [2] Blair, W.D, J.E Gray, and M.D Boyd. (1991). "Design Analysis for the Two-Stage Alpha, Beta, Gamma Estimator." 1050. Print.
- [3] Brookner, E. (1998). *Tracking and Kalman filtering made easy*. New York, Wiley.
- [4] Gray J. E. & Murray W. J. (1993). "A Derivation of an Analytic Expression for the Tracking Index for the α - β - γ Filter." IEEE Trans. On Aerospace and Electronic Systems, Vol. 29, no. 3.
- [5] Jury, E. I. (1964). "Theory and application of the z-transform method". New York, Wiley, p. 93.
- [6] Kalata P. R. (1984). "The tracking index: A generalized parameter for α - β and α - β - γ target tracker," IEEE Trans. on Aerospace and Electronic Systems, AES-20, 2, pp. 174-181.
- [7] Mahafza, B. R., & A. Z., Elsherbeni. (2004). MATLAB simulations for radar systems design. Boca Raton, FL: CRC Press/Chapman & Hall.
- [8] Njonjo A.W., Pan B.F. & Jong T.G. (2016). "A Basic Study on Development of a Tracking Module for ARPA system for Use on High Dynamic Warships," Journal of Navigation and Port Research Vol.40 No.2 pp.83-87
- [9] Pan B.F., Njonjo A.W. & Jong T.G. (2016). "Basic Study of the Optimization of the Gain Parameters α , β and γ of a Tracking Module for ARPA system on Board High Dynamic Warships," Journal of Navigation and Port Research Vol.40 No.5 pp.241-247.

- [10] Simpson, H. R. (April 1963). “Performance Measures and Optimization Condition for a Third Order Sampled-Data Tracker,” IEEE Transactions on Automatic Control, Vol. AC8, pp. 182–183.
- [11] Tenne D. & T. Singh. (2002). “Characterizing performance of α - β - γ filters,” IEEE Transactions on Aerospace and Electronic Systems, vol. 38, no. 3, pp. 1072–1087.



Acknowledgements

It has been nearly two years since I came to South Korea to pursue a Master's degree and I cannot begin to express my gratitude for being availed the opportunity to study at Korea Maritime and Ocean University. However, the journey has not been without challenges and for this I would like to acknowledge several people for their support, advice and assistance without whom I could not have made it.

First, I would like to convey my deepest gratitude and sincere appreciation to my advisor and supervisor, Prof. Jeong Tae-Gweon. He has continually guided me throughout this research by providing his unparalleled wisdom through refreshing comments, criticism and passion coupled with his enthusiasm for teaching and life as a whole, which has left me extremely inspired as I prepare to take the next step in my career.

Secondly, I am grateful to Prof. Yea Byeong-Deok and Prof. Moon Serng-Bae, both of who were members of my supervisory committee, for the assistance they accorded me while reviewing this thesis and for providing very constructive criticism pertaining to my research. The questions raised and recommendations suggested regarding this thesis not only served to improve it but also assisted in increasing my understanding of the topic investigated in this study.

I wish to also extend my utmost appreciation to my colleague and laboratory mate, Mr. Pan BaoFeng. This thesis could not have been possible without his brilliant ideas, persistent help and support. He has shown me unmatched kindness and care as well as being an anchor that I could always count on during my stay in Korea.

I would also like to thank all the professors in the College of Maritime Science at Korea Maritime and Ocean University for all the assistance and advice I received from them during my study period in the department of Navigation Science. I have learnt a great deal from them including Korean culture and I sincerely hope to use the knowledge I have gained to impact positively in my home country Kenya.

In addition, I am thankful to Korea Maritime and Ocean University and Jomo Kenyatta University of Agriculture and Technology for the combined effort in ensuring that I had all the support I needed to study and realize this goal. I hope to utilize this opportunity to promote strong socio- economic ties between Korea and Kenya.

Also, I am heavily indebted to my husband and son, Arthur, for whom my love and admiration grows exponentially with each passing day. I sincerely thank them for their patience and inspiration throughout these two years. They have been my rock, my biggest fans and have provided the motivation I needed to come this far.

And above all, I attribute all my success and achievements thus received to the Almighty God for keeping me in good health and providing the strength I needed each step of the way. May all the glory, honor and power be unto Him.